Stable and Functional Expression of the ClC-3 Chloride Channel in Somatic Cell Lines

Masanobu Kawasaki,* Makoto Suzuki,†
Shinichi Uchida,* Sei Sasaki,* and Fumiaki Marumo*
*Second Department of Internal Medicine
School of Medicine
Tokyo Medical and Dental University
Bunkyo-ku, Tokyo 113
Japan
†Department of Pharmacology
Jichi Medical College
Tochigi 329-04
Japan

Summary

The ClC family is the superfamily of voltage-gated Cl⁻ channels. Although the ClC channels expressed in Xenopus oocytes have been characterized, their channel properties are still poorly understood. We recently cloned a unique member of the ClC family, ClC-3, that is expressed abundantly in neurons. Its channel activity was regulated by phorbol esters. Now, we have established a stably transfected somatic cell line expressing functional ClC-3 channels and examined the ClC-3 single-channel current by patch-clamp techniques. In inside-out patches from the stably transfected cells, a rise of bath Ca^{2+} concentration in the physiological range of intracellular Ca^{2+} concentrations inhibited the ClC-3 single-channel currents. This inhibition by Ca^{2+} was independent of phosphorylation and ATP. Thus, the ClC-3 channel is a Ca^{2+}-sensitive Cl⁻ channel localized in neuronal cells, and its Ca^{2+} sensitivity implies a physiological role in neuronal functions.

Introduction

Recently, several members of the ClC family have been cloned. The ClC family consists of six members: ClC-0, ClC-1, ClC-2, ClC-3, ClC-K1, and ClC-K2 (Jentsch et al., 1990; Steinmeyer et al., 1991; Thiemann et al., 1992; Kawasaki et al., 1994; Uchida et al., 1993; Adachi et al., 1994). These members appear to share 12 or 13 membrane-spanning domains, and all of them except for ClC-3 share about 40% amino acid identity. The ClC-3 channel is an intriguing member of the ClC family. Only 20%–24% of the amino acid sequence encoded by ClC-3 is identical to those of other cloned ClC Cl⁻ channels. Although the ClC-3 cDNA was isolated from a rat kidney cDNA library, its expression was abundant in rat brain, especially in the neuronal cells in the hippocampus, in the olfactory bulb, and in the Purkinje cells in the cerebellum (Kawasaki et al., 1994). The Cl⁻ current elicited by ClC-3 in Xenopus oocytes was completely blocked by phorbol esters. The currents were examined by two-microelectrode voltage-clamp techniques in Xenopus oocytes injected with in vitro transcribed ClC-3 cRNAs (Kawasaki et al., 1994).

To examine the physiological, biochemical, and phar-macological properties of the ClC-3 channels in more detail, we established a stably transfected mammalian cell line expressing functional ClC-3 Cl⁻ channels. Single-channel recordings allow the direct observation of the fundamental properties of individual ion channels. We therefore characterized the single-channel behavior of the cloned ClC-3 channel using a patch-clamp technique.

Results

Transfection and Expression of ClC-3 in CHO Cells

Chinese hamster ovary cells (CHO-K1) were stably transfected with the coding sequence of cloned rat kidney ClC-3 using a dexamethasone-inducible expression vector, pMAM-neo (Lee et al., 1981; Chen and Okayama, 1987; Tabcharani et al., 1991). After the selection with G418 for 5 months, 75 clonal cell lines derived from the transfected cells were examined for ClC-3 mRNA. Figure 1A shows a Northern blot of total RNA isolated from a series of clonal cell lines probed with ³²P-labeled ClC-3 cDNA. We obtained only one clonal cell line (C21) that expressed a 3.5 kb mRNA (ClC-3) upon treatment of 2 μM dexamethasone. To examine the expression of ClC-3 channels on the cell surface, we assayed the C21 cells by the patch-clamp technique in the whole-cell configuration. C21 cells generated outward currents (2535 ± 176 pA; mean ± SEM at +10 mV membrane potential; n = 10), but nontransfected CHO-K1 cells did not produce a similar level of current amplitude (14 ± 4 pA; n = 10; Figure 1B). When membrane voltages were held at beyond ± 14 mV, these voltage clamps evoked huge currents that induced cell death. Expression of large outward currents was observed in all C21 cells, and it was constantly present through more than 10 passages. In our previous report, we showed the inhibitory effect of 12-O-tetradecanoylphorbol 13-acetate (TPA) on ClC-3 currents expressed in Xenopus oocytes (Kawasaki et al., 1994). In the present study, effect of TPA on the currents expressed in C21 cells was examined in the whole-cell configuration. Treatment of 1 μM TPA for 1 min blocked the currents (120 ± 50 pA; n = 6; Figure 1B, TPA(+)), and this effect was sustained for at least 5 min after the removal of TPA from the bath solution. The inhibitory effect of TPA was completely abolished by cotreatment with 10 μM H-7, which is an inhibitor of protein kinases (2743 ± 194 pA; n = 6; Figure 1B, TPA(+) and H-7(+)). We also examined the inhibitory effect of 4,4'-diisothiocyanatostilbene-2,2'-disulphonic acid (DIDS) on the ClC-3 whole-cell currents. Treatment of 1 mM DIDS blocked the currents (40 ± 26 pA; n = 6). These properties of the whole-cell currents were consistent with the previous data from the two-microelectrode voltage-clamp studies in Xenopus oocytes (Kawasaki et al., 1994).

To characterize the single-channel properties of the ClC-3 Cl⁻ channel, we applied the conventional patch-clamp technique to the C21 cells and obtained ClC-3 single-channel recordings. Underlying small conductance Cl⁻ channels of ~30 pS (Reinhardt et al., 1987; Gabriel et

A

Control		Clone 21	
Lane1	Lane2	Lane3	Lane4

-28S

-18S

B

Control CHO⁻

TPA(-)

TPA(+)

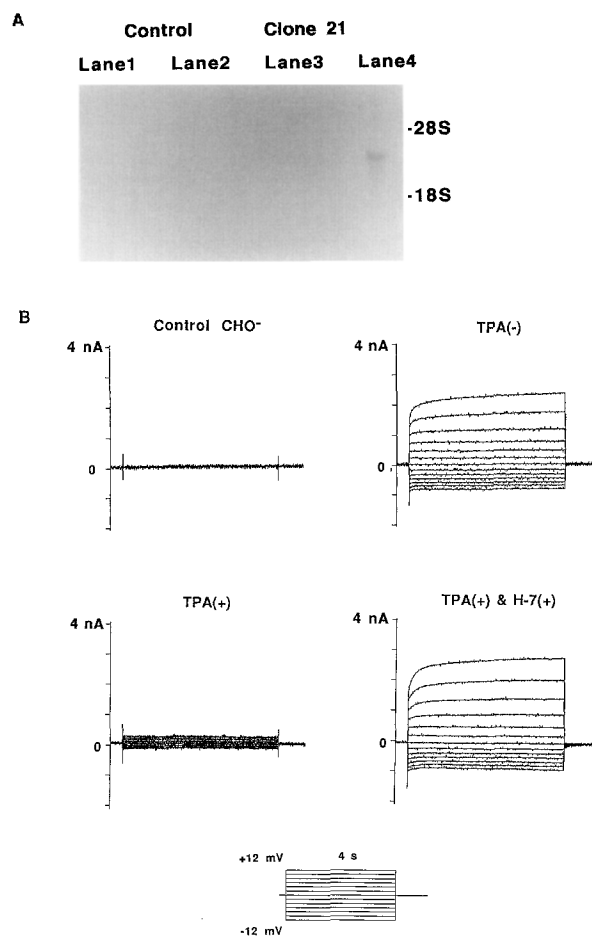TPA(+) & H-7(+)

+12 mV   4 s

-12 mV

Figure 1. Expression of ClC-3 in CHO Cells

(A) Northern blot analysis of transfected cells. CHO control indicates the total RNA was isolated from the cells transfected with a expression vector only; dex (+), pretreatment with 2 μM dexamethasone for 2 days; dex (−), without the pretreatment. Lane 1, control dex (−); lane 2, control dex (+); lane 3, clone 21 Dex (−); lane 4, clone 21 Dex (+). A lane on an agarose gel contained 10 μg of total RNA from each transfected cell line.

(B) Traces of whole-cell currents from C21 cells. Control CHO⁻, nontransfected CHO cells; TPA(+), treatment with 1 μM TPA; TPA(−), without the treatment; TPA(+)&H-7(+), cotreatment with 1 μM TPA and 10 μM H-7. The holding potential was changed from −12 to +12 mV.

A

Vm(mV)

-20--60

-10

0

+10

+20

+40

+60

Current (pA)

10

5

-60 -40 -20 0 20 40 60 Vm (mV)

-5

10 pA

100 msec

B

10 sec.

10 pA

S0
S2
S1

C

Current (pA)

10

8

6

4

2

-40   -20   0   20   40   60   80
Vm(mV)

-2

I   Br   F

Figure 2. Single-Channel Properties of ClC-3 Channels

(A) Tracings and current–voltage relation of inside-out patches in symmetrical 120 mM Cl⁻. The pipette Ca^{2+} concentration was 1 mM; the bath Ca^{2+} concentration was nominally Ca^{2+}-free. Ensemble averages of ClC-3 channel currents were constructed for each of the data points plotted. Voltage was ramped from −60 mV to +60 mV. Circles, ClC-3 (S2) inside-out patch clamp recordings (n = 10); arrows, closed state of channels. Outward currents are negative.

(B) Traces of the ClC-3 single-channel recording. S1, the high conductance Cl⁻ current; S2, the middle conductance Cl⁻ current. After the patch-membrane was detached from the cell to form the excised inside-out patch, membrane potential was maintained at +40 mV at bath Ca^{2+} concentration of 10 nM.

(C) Current–voltage relationships in the half replacement with other anions. The single-channel conductances were measured between 0 and +40 mV. Ensemble averages of ClC-3 channel currents were constructed for each of the data points plotted (n = 3). The pipette solution contained 120 mM NaCl. The bath solution for F was 60 mM NaCl and 60 mM NaF; for Br, 60 mM NaCl and 60 mM NaBr; and for I, 60 mM NaCl and 60 mM NaI.

al., 1992; Bear, 1994) were found in wild-type CHO-K1 cells in cell-attached and inside-out patches at positive membrane voltage (37.5%; 12 of 32; data not shown). The currents elicited by ClC-3 cDNA were not found in the cell-attached patches from C21 cells. However, when the membrane potential was maintained at +60 mV after detaching the patched membrane from the C21 cell at 10 nM bath Ca^{2+} concentration, a large Cl⁻ current appeared with a variable time course (run-up within 0.5–3 min; n = 78 of 100). Although the large-conductance Cl⁻ currents appeared in inside-out patches from the C21 cells, they never appeared in the patches from wild-type CHO-K1 cells and CHO-K1 cells transfected with a noninsert vector and cultured with dexamethasone (n = 0 of 50). Without treatment of dexamethasone, the C21 cells
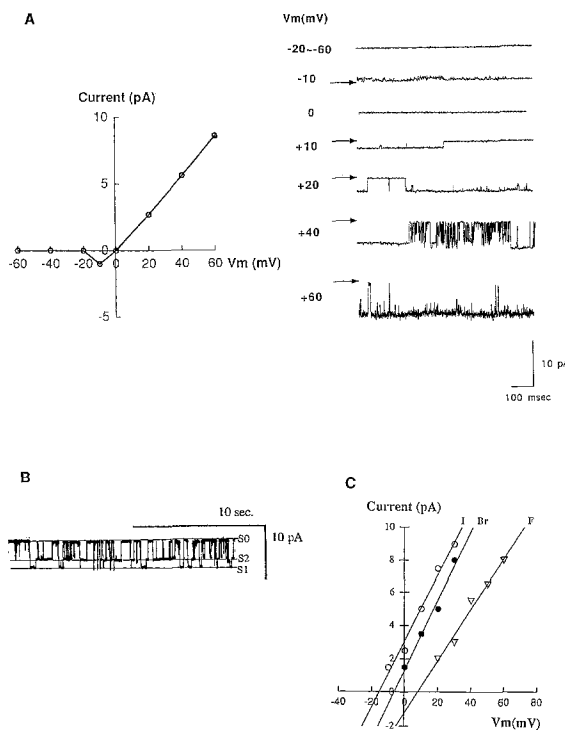
weakly expressed ClC-3 mRNA in an overexposed Northern blot, and the probability of the appearance of the large Cl⁻ channel decreased (n = 18 of 50). Based on these data, we identified the large Cl⁻ currents with ClC-3 currents.

In the nominally Ca^{2+}-free bathing solution containing 1 mM EGTA, ClC-3 channels passed outward Cl⁻ currents at positive membrane potential, but passed no inward Cl⁻ currents at less than −20 mV membrane potential (Figure 2A). When a patched membrane contained one active channel, the large Cl⁻ channel always had two conductance states of a middle conductance state (S2) and a high conductance state (S1; Figure 2B; pCa 8). In its open state, direct transitions between S1 and S2 were observed at +40 mV membrane potential. In inside-out patches with symmetrical 120 mM Cl⁻ solutions, the conductance states
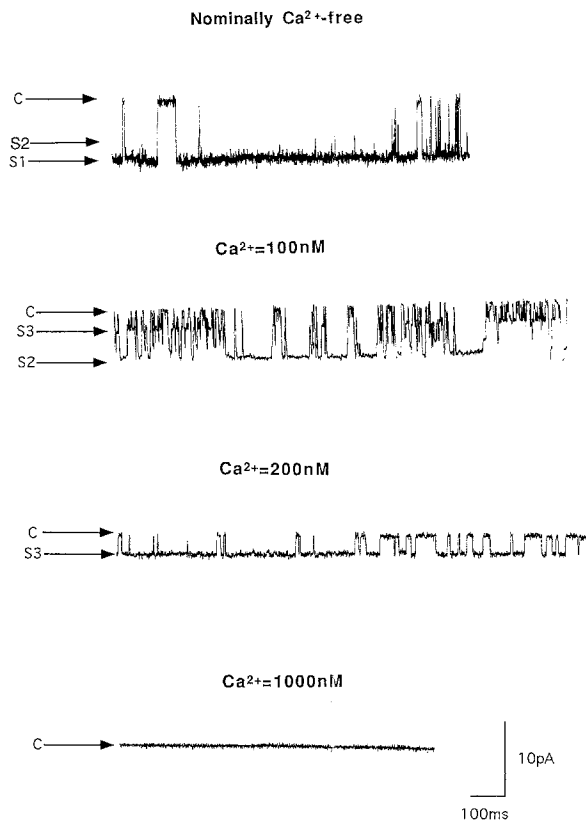
Nominally Ca²⁺-free

Ca²⁺=100nM

Ca²⁺=200nM

Ca²⁺=1000nM

10pA

100ms

Figure 3. Effect of Ca^{2+} on the ClC-3 Channel Currents

Representative stationary-state single-channel traces in a single-channel patch at several Ca^{2+} concentrations in the presence of 10 mM H-7 and 0.2 U/ml alkaline phosphatases. The patched membrane potential was held at +60 mV; data were filtered at 1 kHz. C, closed state of the channel; S1, the high conductance Cl⁻ current; S2, the middle conductance Cl⁻ current; S3, the intermediate conductance Cl⁻ current.

were 100 pS (S2) and 140 pS (S1) for ClC-3 channels. When Cl⁻ was partially replaced with other anions, the best fit of the current equation to data was used to obtain each reversal potential in the Nernst equation. The anion permeability ratio sequence was I⁻ (3.4) > Br⁻ (1.2) > Cl⁻ > F⁻ (0.36) (Figure 2C). Thus, the ClC-3 channel is a patch excision and depolarization-induced outwardly rectifying Cl⁻ channel.

Ca²⁺-Dependent Gating of Recombinant ClC-3 Channels

Since phorbol esters had modified the ClC-3 currents in Xenopus oocytes (Kawasaki et al., 1994), we first tried to examine the effect of protein kinase C on the ClC-3 single channel in the inside-out configuration. Although protein kinase C (0.8 U/ml) with cofactors inhibited the ClC-3 currents, the inhibition was quickly recovered by EGTA treatment (data not shown). From this evidence, we speculated that the Ca^{2+} may be a modulator of ClC-3 channel activity, which is independent of the modulation of protein kinase C. We therefore examined the effect of Ca^{2+} on the channel. Figure 3 shows the effect of bath Ca^{2+} concentrations on the ClC-3 single-channel currents at a membrane po-

tential of +60 mV in inside-out patches. The bath solution contained 10 μM H-7 and 0.2 U/ml alkaline phosphatase, but did not contain ATP. On exposure to the nominally Ca^{2+}-free solution, the main single-channel currents were the large-conductance currents, S1 conductance level (140 pS), but the currents of S2 conductance level (100 pS) were infrequently observed. At 100 nM bathing Ca^{2+} concentration, the main single-channel currents were changed from S1 conductance level to S2 conductance level, and a further small conductance level (40 pS), S3, appeared. Fast direct transitions among three states (closed, S2, and S3) were observed. At 200 nM bathing Ca^{2+} concentration, the main single-channel current was S3 conductance level. Finally, at 1000 nM bathing Ca^{2+} concentration, the ClC-3 single-channel currents disappeared.

Figure 4 shows the effect of changing bath Ca^{2+} concentrations on the ClC-3 currents at 40 mV membrane potential in inside-out patches in the presence of 3 μM staurosporin. Upon formation of an inside-out membrane patch from the C21 cells in 10 nM Ca^{2+} bath solution, spontaneous opening of ClC-3 channels appeared. Its amplitude histogram shows three peaks indicating two current gaps (-4.12 ± 0.29 [S2] and −5.7 ± 0.22 pA [S1], Gaussian analysis; Figure 4, A phase). When bathing Ca^{2+} concentration was increased to 200 nM using the multiple outlet method (Yellen, 1982), the channel currents switched from the large-conductance levels to S3 conductance level (−1.6 ± 0.18 pA [S3], Gaussian analysis, Figure 4, B phase). Further increase in Ca^{2+} concentration to 1 μM shut off the currents (Figure 4). Restoration of the channel activity was sequentially obtained by exposure to a nominally Ca^{2+}-free solution containing 1 mM EGTA (Figure 4).

The above results expected that an increase in intracellular Ca^{2+} concentration inhibits ClC-3 channels in intact cells. This speculation was examined in C21 cells using the whole-cell patch-clamp technique. Figure 5 shows the effect of an elevation of intracellular Ca^{2+} concentration on the whole-cell currents using a Ca^{2+} ionophore, ionomycin. The ClC-3 currents were observed in whole-cell patch-clamp recordings in response to voltage pulse of ± 10 mV. When the patched cell was exposed to 1 μM ionomycin, the magnitude of the whole-cell currents gradually decreased in a few seconds, and its reversal potential was shifted. After a few minutes, the whole-cell currents were completely blocked (n = 3).

Further analysis of the single-channel recordings of ClC-3 channels at various Ca^{2+} concentrations was performed. Figure 6A shows the open probability of S2 state as a function of membrane potential. The open probability was dependent on membrane potential in the presence of bath Ca^{2+}. Voltage endowing S2 half open (P_o = 50%) shifted to the right after increasing bath Ca^{2+} concentration (20 mV at 10 nM, 40 mV at 100 nM, 70 mV at 200 nM). Figure 6B shows the open and closed analysis of ClC-3 channels using the unconditional distributions of these interval durations (Blatz and Magleby, 1986). The data were recorded for 8 min at 10 nM bath Ca^{2+} and +20 mV membrane potential. At this condition, the main conductance state was S2 state, and the probability of S1 state and S3

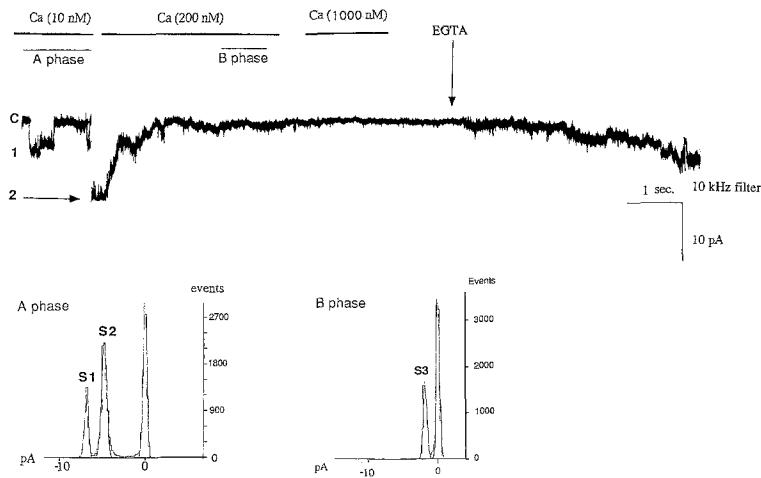Ca (10 nM)   Ca (200 nM)   Ca (1000 nM)
EGTA

A phase   B phase

Figure 4. Effect of Changing Bath Ca^{2+} Concentration on ClC-3 Currents

Representative traces recorded from an inside-out patch containing two channels sequentially exposed to different Ca^{2+} concentrations in the presence of 3 μM staurosporin. Labeled bars indicate changes of bath solutions; the patched membrane potential was held at +40 mV; data were filtered at 10 kHz. C, closed state of the channel; 1, one channel open; 2, two channels open. A phase, the distribution of the amplitudes of single-channel currents at the 10 nM bath Ca^{2+} concentration; B phase, the distribution of the amplitudes of single-channel currents at 200 nM Ca^{2+}. The continuous curves represent the Gaussian distributions fitted to the data by the method of maximum likelihood for A phase and B phase.

state was infrequent. The open (Figure 6B, upper panel) and closed (Figure 6B, lower panel) analyses indicated that the ClC-3 channel at S2 state must have at least three open kinetic states and at least four closed kinetic states; however, the assignment of the best kinetic scheme of ClC-3 channels is not possible at present.

Discussion

This study shows the establishment of a stably transfected cell line of the ClC family. CHO-K1 cells may be favorable for natural expression of rat ClC-3 channels, since chinese hamsters and rats are genetically close. Examination of ClC-3 single-channel recordings provides novel evidence for ion channels. The ClC-3 protein is a Ca^{2+}-sensitive, outwardly rectifying Cl^- channel. A rise of bathing Ca^{2+} concentration flickered out the single-channel currents in the range of physiological intracellular Ca^{2+} concentrations. Its blockade depends on membrane potential and intracellular Ca^{2+} concentrations, but not on the modulation of protein kinases and ATP-dependent processes.

We previously reported that phorbol esters blocked the ClC-3 currents expressed in Xenopus oocytes (Kawasaki

et al., 1994). In this study, the ClC-3 transfected mammalian cell line generated an outward current in the whole-cell configuration, and this current was also inhibited by phorbol esters. These results showed that the cell line expressing ClC-3 channels was established, and the regulation of the ClC-3 channel by phorbol esters was conserved when expressed in the rodent and amphibian cells.

The ClC-3 channel is a large-conductance Cl^- channel. Based on the reversal potential at partial Cl^- replacements with other anions, we determined that the anion permeability ratio sequence was $I^- > Br^- > Cl^- > F^-$ (see Figure 2C). Our previous study in Xenopus oocytes showed the similar anion permeability ratio sequence, $I^- > Br^- = Cl^-$ (Kawasaki et al., 1994). A small discrepancy may be due to some endogenous currents present in Xenopus oocytes. This sequence is compatible with Eisenman's series 1 (Diamond and Wright, 1969), suggesting that the ClC-3 protein may have a binding site with a low positive charge and have a pore with relatively large radius compared with other Cl^- channels. Therefore, its large conductance may be related to its pore size.

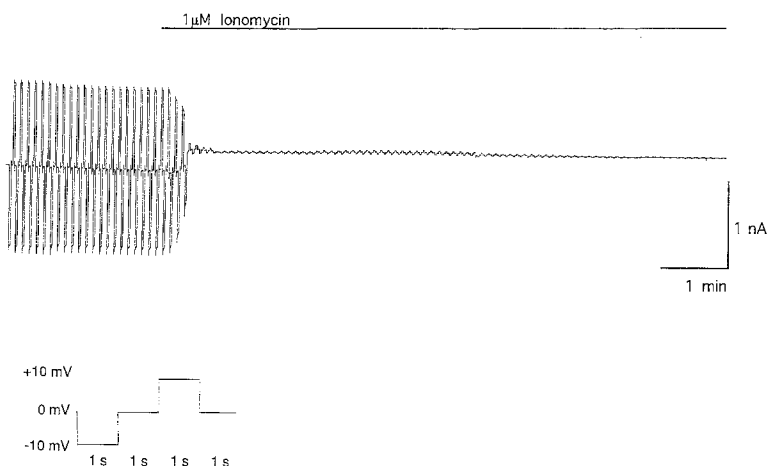The ClC-3 channel is a patch excision and depolarization-induced channel. Although the channel currents did

1 μM Ionomycin

Figure 5. Representative Traces of Whole-Cell Currents from C21 Cells Exposed to a Ca^{2+} Ionophore, 1 μM Ionomycin

Labeled bars indicate changes of bath solutions. The holding potential was clamped at ± 10 mV.

+10 mV
0 mV
-10 mV
1 s   1 s   1 s   1 s

A

B

Proportion (P)	Scaling Factor	τ(ns)
0.439	791.331	0.459
0.323	581.285	2.485
0.238	428.628	15.566

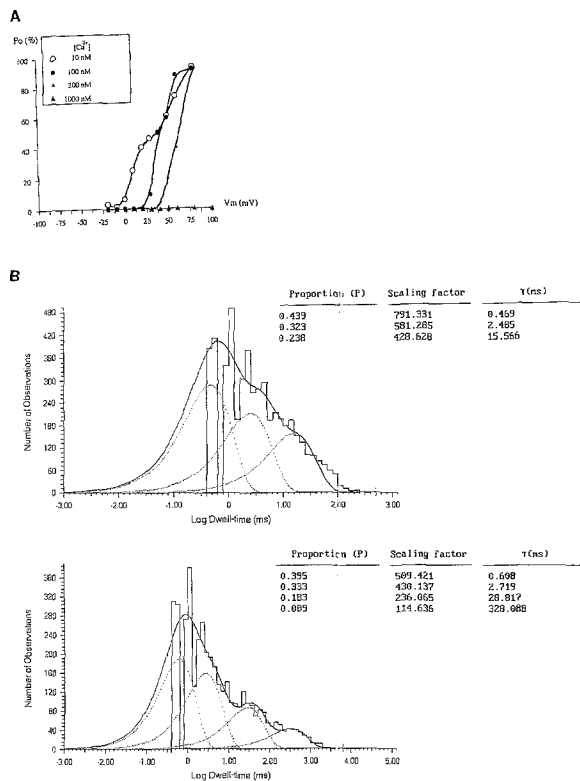| Proportion (P)	Scaling Factor	τ(ns)
0.395	509.421	0.698
0.333	430.137	2.719
0.183	236.065	28.817
0.089	114.636	328.688

Figure 6. Functional Analysis of ClC-3 Channels

(A) Voltage dependence of ClC-3 S2 open-channel probability at concentrations of 10 nM (open circles), 100 nM (closed circles), 200 nM (open triangles), and 1000 nM (closed triangles) Ca^{2+}. Open-channel probability in a patch for each voltage and Ca^{2+} concentration was determined as the average P_o percentage of 10 s duration. These Ca^{2+} concentrations of the bathing solutions were measured using Fura2 fluorescence.

(B) Fitting analysis of the ClC-3 S2 currents. The data of the single-channel currents at +20 mV membrane potential for 8 min were analyzed. Upper, open state; lower, closed state.

not appear in the cell-attached mode, the ClC-3 channels became active in the cell-free mode. Previous physiological studies demonstrated the excision activation of other Cl^- channels (Hanrahan et al., 1985; Krouse et al., 1989). It is speculated that cytosolic inhibitory factors may exist in the cell and inhibit the Cl^- channels (Kunzelmann et al., 1991; Krick et al., 1991). In our cell-attached studies, the transfected cells were washed with the bath solution, and patched membranes were pulled into a patch pipette by suction. It may be possible that this handling produces shear stress, and that the shear stress elevates intracellular Ca^{2+} concentration and activates protein kinase C (Shen et al., 1992; Nollert et al., 1990). The cytosolic changes induced by shear stress may inhibit the ClC-3 channels in cell-attached patches. Detaching the patched membrane from the cell sets the ClC-3 channels free from cytosolic components and decreases the Ca^{2+} concentration on the intracellular surface of the ClC-3 channels. The decrease of the Ca^{2+} concentration may activate the ClC-3 channel. Further studies on the properties of the ClC-3

channel may clarify the activation mechanisms of patch excision and depolarization-induced Cl^- channels.

Many investigators have reported on the Ca^{2+}-dependent activation mechanisms of ion channels, Ca^{2+}-activated K^+ channels (Atkinson et al., 1991), and Ca^{2+}-activated Cl^- channels (Owen et al., 1984; Mayer, 1984). However, there have been two reports on Ca^{2+}-dependent inactivation mechanisms, namely, a report on GABA receptors (Inoue et al., 1986) and a report on the Ca^{2+} channel (Johnson and Byerly, 1993; Imredy and Yue, 1994). The inhibition of ClC-3 channel is another type of Ca^{2+}-dependent inactivation mechanism of ion channels. When the excised patches were exposed to Ca^{2+} concentrations corresponding to the physiological range of intracellular Ca^{2+} concentrations, the ClC-3 channels made fast transitions among four conductance levels, S1, S2, S3, and closed. A similar half-blocking phenomenon was previously reported in IRK1 channels, in which Mg^{2+} block induced sublevels of conductance (Matsuda, 1988; Matsuda et al., 1989). Our study showed a new type of half-blocking mechanism induced by Ca^{2+}. In the nominally Ca^{2+}-free solution, the main single-channel conductance level was S1 state, full conductance. The Ca^{2+} concentration of 10 nM changed the main single-channel conductance level from full conductance level to S2, a lower conductance level. In the presence of 100 nM bathing Ca^{2+} concentration, single channels began to show fast transitions to another lower conductance level, S3 (40 pS). The Ca^{2+} concentration of 200 nM changed the main conductance level from S1/S2 conductance level to S3. Increasing bath Ca^{2+} concentration up to 1 μM inactivated the channel at any given membrane potential.

S3 conductance level was not derived from endogenous Cl^- channels, since it always appeared after S1/S2 conductance levels when the bath Ca^{2+} concentration was elevated more than 100 nM (100%; n = 30 of 30). Excised patches from wild-type CHO cells revealed mainly the underlying Cl^- conductance of ~30 pS (Reinhardt et al., 1987; Gabriel et al., 1992; Bear, 1994). Therefore, Ca^{2+} concentrations that correspond to a physiological range of intracellular Ca^{2+} concentrations induce the conductance switching among four conductance levels in ClC-3 channels. Alterations of the conductance levels (S2–S3/S1–S2) by Ca^{2+} were probably due to subconductance states of the ClC-3-encoded Cl^- channel. It is, however, not certain whether the alteration is due to the switching of the triple-barreled channel. Because some Cl^- channels, including ClC-0, are known to encode double barrels (Miller and White, 1984), a hypothesis of a triple-barreled channel cannot be neglected.

The ClC-3 channel also belongs to a member of the voltage-gated Cl^- channels. The open probability of ClC-3 channels depends on membrane potential in the presence of bath Ca^{2+}. A similar mechanism underlying this phenomenon, which is well defined in N-methyl-D-aspartate (NMDA) receptors (Nowak and Prochiantz, 1984; Mayer et al., 1984) and K^+ channels, is the (Matsuda et al., 1987; Horie et al., 1987; Vandenberg, 1987) so-called flickering block by Mg^{2+}. Previous studies on the mechanism of flickering block by Mg^{2+} indicated that the flickering may be

due to an inherent kinetic property of the K^+ channel rather than direct occlusion by Mg^{2+} (Horie et al., 1987). A point mutation study on NMDA receptors suggested that they possess a Mg^{2+} binding site (Mori et al., 1992). Intracellular Ca^{2+} may be a inhibitory ligand for ClC-3 channels, just as Mg^{2+} is for these channels.

This Ca^{2+}-sensitive Cl^- channel is dominantly expressed in excitable cells. Our in situ hybridization study showed that the ClC-3 mRNA was abundantly expressed in neuronal cells in the hippocampus, the olfactory bulb, and the cerebellum (Kawasaki et al., 1994). In these locations, intracellular Ca^{2+} ions play a vital role in the neuronal functions, synaptic plasticity (Lynch et al., 1983; Malenka et al., 1988; Perkel et al., 1993; Wyllie et al., 1994), and olfactory transduction (Kleene, 1993; Kurahashi and Yau, 1993; Lowe and Gold, 1993). Recently, ClCN4, which is strikingly similar to ClC-3, was isolated from the human Xp22.3 region using positional cloning strategy (van Slegtenhorst et al., 1994). A male patient who possessed a partial deletion of ClCN4 suffered from delays in psychomotor functions and mental retardation. These clinical features may have been induced by the loss of ClCN4 function. Possibly, the ClC-3 gene is a rat homolog of the human ClCN4. Further studies on the neuronal functions of the ClC-3 channel are clearly needed.

Experimental Procedures

Transfection
Plasmid Constructions
The cDNA of rat ClC-3 Cl^- channel was originally ligated into plasmid pSPORT1. We made the encoding ClC-3 fragment with SalI (5') and blunt (3') restriction sites. The SalI and blunt cut fragment was ligated into a mammalian expression vector, pMAM-neo (Lee et al., 1981), at the SalI and blunt sites and propagated in Escherichia coli.
Cell Culture and Transfection
CHO-K1 (wild-type) cells (obtained from JCRB) were grown in Ham's F12 Nutrient Mix (Gibco) supplemented with 10% fetal bovine serum at 37°C in 5% CO_2. Conventional transfection was carried out using a mammalian transfection kit ($CaPO_4$; Stratagene). Cells containing stably integrated copies of transfected recombinant plasmid were selected by adding Geneticin (G418, Life Technologies) to the growth media at a concentration of 700 μg/ml. After selection for 5 months, G418-resistant cell clones were isolated and transferred to separate culture dishes for expansion and analysis.
Northern Blot Analysis
Total RNA was isolated from about 10^7 cells of each G418-resistant clone treated with or without 2 μM dexthamethasone for 24 hr. Each sample of total RNA (20 μg) was resolved in a formaldehyde/0.7% agarose gel and blotted overnight onto a nylon membrane. The RNA was cross-linked to the membrane by ultraviolet light, prehybridized for 2 hr in a solution containing 6× SSPE solution, 5× Denhart's solution, 50% formamide, 2% SDS, and 100 μg/ml of denatured salmon sperm DNA at 65°C, and hybridized overnight with 10^6 cpm/ml of ClC-3 cDNA probe labeled with [α-^{32}P]dCTP (Amersham) by random priming (Promega). After hybridization, the membrane was washed twice in 2× SSC, 0.1% SDS at room temperature, and once with 0.1 × SSC, 0.1% SDS at 65°C for 30 min. Hybridization was visualized by autoradiography.

Electrophysiological Characterization
Conventional patch-clamp techniques were used to record single-channel currents and whole-cell currents from ClC-3-transfected CHO cells. Currents were recorded at room temperature (20°C–24°C) with an EPC-7 patch-clamp amplifier (List-Electronic, West Germany), and the data were stored on a DAT recorder (DAT-200, Sony, Tokyo). Re-

cords were sampled at 2000 points per second and analyzed on a Compaq ProLinea 4/50 computer using Axon version 5.5.1 software. The obtained data were transferred to a Macintosh SE/30 computer and analyzed using Excel 2.2 software. The standard pipette solution contained 120 mM NMDG–Cl, 1 mM $MgCl_2$, 10 mM PIPES, 1 mM EGTA, and 0.51 mM $CaCl_2$ (pH 7.30). The standard bath solution contained 120 mM NMDG–Cl, 1 $MgCl_2$, 10 mM PIPES, 1 mM EGTA, and 0.09 mM $CaCl_2$ (pH 7.30). In the whole-cell configuration, the pipette solution contained 130 mM K–gluconate, 20 mM KCl, 5 mM PIPES, 1 mM EGTA, and 100 μg/ml nystatin (stock solution, 25 mg/ml in dimethyl sulfoxide; Levitan and Kramer, 1990) (pH 7.20). The bath solution contained 130 mM tetraethylammonium chloride, 1 mM $MgCl_2$, 10 mM PIPES, 1 mM EGTA, and 0.51 mM $CaCl_2$ (pH 7.40). The ionomycin solution contained 130 mM TEA-Cl, 1 mM $MgCl_2$, 10 mM PIPES, 1 mM EGTA, 0.51 mM $CaCl_2$, and 1 μM ionomycin (stock solution, 1 μM in dimethyl sulfoxide; Calbiochem). The Ca^{2+} concentrations of the bath solutions were measured using a fluorescent indicator Fura2 (Williams et al., 1985; Iino et al., 1990). Data were usually filtered at 1 kHz and sampled at 2 kHz. In Figure 3B, data were filtered at 10 kHz to reveal the fast switching of conductance levels.

References

Adachi, S., Uchida, S., Hata, M., Ito, H., Hiroe, M., Marumo, F., and Sasaki, S. (1994). Two isoforms of a chloride channel predominantly expressed in thick ascending limb of Henle's loop and collecting ducts of rat kidney. J. Biol. Chem. 269, 17677–17683.

Atkinson, N. S., Robertson, G. A., and Ganetzky, B. (1991). A component of calcium-activated potassium channels encoded by the Drosophila slo locus. Science 253, 551–555.

Bear, C. E. (1994). Drugs transported by p-glycoprotein inhibit a 40 pS outwardly rectifying chloride channel. Biochem. Biophys. Res. Commun. 200, 513–521.

Blatz, A. L., and Magleby, K. L. (1986). Quantitative description of three models of activity of fast chloride channels from rat skeletal muscle. J. Physiol. 378, 141–174.

Chen, C., and Okayama, H. (1987). High-efficiency transformation of mammalian cells by plasmid DNA. Mol. Cell. Biol. 7, 2745–2752.

Diamond, J. M., and Wright, E. M. (1969). Biological membranes: the physical basis of ion and nonelectrolyte selectivity. Annu. Rev. Physiol. 31, 581–646.

Gabriel, S. E., Price, E. M., Boucher, R. C., and Stutts, M. J. (1992). Small linear chloride channels are endogenous to nonepithelial cells. Am. J. Physiol. 70, 708–713.

Hanrahan, J. W., Alles, W. P., and Lewis, S. A. (1985). Single anion-selective channels in basolateral membrane of a mammalian tight epithelium. Proc. Natl. Acad. Sci. USA 82, 7791–7795.

Horie, M., Irisawa, H., and Noma, A. (1987). Voltage-dependent magnesium block of adenosine-triphosphate-sensitive potassium channel in guinea-pig ventricular cells. J. Physiol. 387, 251–272.

Iino, M., Ozawa, S., and Tsuzuki, K. (1990). Permeation of calcium through excitatory amino acid receptor channels in cultured rat hippocampal neurones. J. Physiol. 424, 151–165.

Imredy, J. P., and Yue, D. T. (1994). Mechanism of Ca^{2+}-sensitive inactivation of L-type Ca^{2+} channels. Neuron 12, 1301–1318.

Inoue, M., Oomura, Y., Yakushiji, T., and Akaike, N. (1986). Intracellular calcium ions decrease the affinity of the GABA receptor. Nature 324, 156–158.

Jentsch, T. J., Steinmeyer, K., and Schwarz, G. (1990). Primary structure of Torpedo marmorata chloride channel isolated by expression cloning in Xenopus oocytes. Nature 348, 510–514.

Johnson, B. D., and Byerly, L. (1993). A cytoskeletal mechanism for Ca²⁺ channel metabolic dependence and inactivation by intracellular Ca²⁺. Neuron 10, 797–804.

Kawasaki, M., Uchida, S., Monkawa, T., Miyawaki, A., Mikoshiba, K., Marumo, F., and Sasaki, S. (1994). Cloning and expression of a protein kinase C–regulated chloride channel abundantly expressed in rat brain neuronal cells. Neuron 12, 597–604.

Kleene, S. J. (1993). Origin of the chloride current in olfactory transduction. Neuron 11, 123–132.

Krick, W., Disser, J., Hazama, A., Burckhardt, G., and Froemter, E. (1991). Evidence for a cytosolic inhibitor of epithelial chloride channels. Pflügers Arch. 418, 491–499.

Krouse, M. E., Hagiwara, G., Chen, J., Lewiston, N. J., and Wine, J. J. (1989). Ion channels in normal human and cystic fibrosis sweat gland cells. Am. J. Physiol. 257, 129–140.

Kunzelmann, K., Tilmann, M., Hansen, C. P., and Greger, R. (1991). Inhibition of epithelial chloride channels by cytosol. Pflügers Arch. 418, 479–490.

Kurahashi, T., and Yau, K. (1993). Coexistence of cationic and chloride components in odorant-induced current of vertebrate olfactory receptor cells. Nature 363, 71–74.

Lee, F., Mulligan, R., Berg, P., and Ringold, G. (1981). Glucocorticoids regulated expression of dihydrofolate reductase cDNA in mouse mammary tumor virus chimaeric plasmids. Nature 294, 228–232.

Levitan, E. S., and Kramer, R. H. (1990). Neuropeptide modulation of single calcium and potassium channels detected with a new patch clamp configuration. Nature 348, 545–547.

Lowe, G., and Gold, G. H. (1993). Nonlinear amplification by calcium-dependent chloride channels in olfactory receptor cells. Nature 366, 283–286.

Lynch, G., Larson, J., Kelso, S., Barrionuevo, G., and Schottler, F. (1983). Intracellular injections of EGTA block induction of hippocampal long-term potentiation. Nature 305, 719–721.

Malenka, R. C., Kauer, J. A., Zucker, R. S., and Nicoll, R. A. (1988). Postsynaptic calcium is sufficient for potentiation of hippocampal synaptic transmission. Science 242, 81–84.

Matsuda, H., Saigusa, A., and Irisawa, H. (1987). Ohmic conductance through the inwardly rectifying K⁺ channel and blocking by internal Mg²⁺. Nature 325, 156–159.

Matsuda, H. (1988). Open-state substructure of inwardly rectifying potassium channels revealed by magnesium block in guinea-pig heart cells. J. Physiol. 397, 237–258.

Matsuda, H., Matsuura, H., and Noma, A. (1989). Triple-barrel structure of inwardly rectifying K channels revealed by Cs and Rb block in guinea-pig heart cells. J. Physiol. 413, 139–157.

Mayer, M. L. (1984). A calcium-activated chloride current generates the after-depolarization of sensory neurons in culture. J. Physiol. 364, 217–239.

Mayer, M. L., Westbrook, G. L., and Guthrie, P. B. (1984). Voltage-dependent block by Mg²⁺ of NMDA responses in spinal cord neurons. Nature 309, 261–263.

Miller, C., and White, M. M. (1984). Dimeric structure of single chloride channels from Torpedo electroplax. Proc. Natl. Acad. Sci. USA 81, 2772–2775.

Mori, H., Masaki, H., Yamakura, T., and Mishina, M. (1992). Identification by mutagenesis of a Mg²⁺-block site of the NMDA receptor channel. Nature 358, 673–675.

Nollert, M. U., Eskin, S. G., and McIntire, L. V. (1990). Shear stress increases inositol triphosphate levels in human endothelial cells. Biochem. Biophys. Res. Commun. 170, 281–287.

Nowak, L., and Prochiantz, A. (1984). Magnesium gates glutamate-

activated channels in mouse central neurones. Nature 307, 462–465.

Owen, D. G., Segal, M., and Barker, J. L. (1984). A Ca²⁺-dependent Cl⁻ conductance in cultured mouse spinal neurones. Nature 311, 567–570.

Perkel, D. J., Petrozzino, J. J., Nicol, R. A., and Connor, J. A. (1993). The role of Ca²⁺ entry via synaptically activated NMDA receptors in the induction of long-term potentiation. Neuron 11, 817–823.

Reinhardt, R., Bridges, R. J., Rummel, W., and Lindemann, B. (1987). Properties of an anion-selective channel from rat colonic enterocyte plasma membranes reconstituted into planar phospholipid bilayers. J. Membr. Biol. 95, 47–54.

Shen, J., Luscinskas, F. W., Connolly, A., Dewey, C. F., Jr., Gimbrone, M. A., Jr. (1992). Fluid shear stress modulates cytosolic free calcium in vascular endothelial cells. Am. J. Physiol. 262, 384–390.

Steinmeyer, K., Ortland, C., and Jentsch, T. J. (1991). Primary structure and functional expression of a developmentally regulated skeletal muscle chloride channel. Nature 354, 301–304.

Tabcharani, J. A., Chang, X. B., Riodan, J. R., and Hanrahan, J. W. (1991). Phosphorylation-regulated Cl⁻ channel in CHO cells stably expressing the cystic fibrosis gene. Nature 352, 628–631.

Thiemann, A., Grunder, S., Pusch, M., and Jentsch, T. J. (1992). A chloride channel widely expressed in epithelial and non-epithelial cells. Nature 356, 57–60.

Uchida, S., Sasaki, S., Furukawa, T., Hiraoka, M., Imai, T., Hirata, Y., and Marumo, F. (1993). Molecular cloning of a chloride channel that is regulated by dehydration and expressed predominantly in kidney medulla. J. Biol. Chem. 268, 3821–3824.

Vandenberg, C. A. (1987). Inward rectification of a potassium channel in cardiac ventricular cells depends on internal magnesium ions. Proc. Natl. Acad. Sci. USA 84, 2560–2564.

van Slegtenhorst, M. A., Bassi, M. T., Borsani, G., Wapenaar, M. C., Ferrero, G. B., Conciliis, L., Rugarli, E. I., Grillo, A., Franco, B., Zoghbi, H. Y., and Ballabio, A. (1994). A gene from the Xp22.3 region shares homology with voltage-gated chloride channels. Hum. Mol. Genet. 3, 547–552.

Williams, D. A., Fogarty, K. E., Tsien, R. Y., and Fay, F. S. (1985). Calcium gradients in single smooth muscle cells revealed by the digital imaging microscope using Fura-2. Nature 318, 558–561.

Wyllie, D. J. A., Manabe, T., and Nicoll, R. A. (1994). A rise in postsynaptic Ca²⁺ potentiates miniature excitatory postsynaptic currents and AMPA responses in hippocampal neurons. Neuron 12, 127–138.

Yellen, G. (1982). Single Ca²⁺-activated nonselective cation channels in neuroblastoma. Nature 296, 357–359.